

MULTI-STAGE OPTIMAL CONTROL OF LIGNOCELLULOSIC BIOETHANOL PRODUCTION

F. DUARTE[‡], G.L. JORIS[‡], A.J. BECCARIA[‡] and R.G. DONDO^{†‡}

[†] Instituto de Desarrollo Tecnológico para la Industria Química (INTEC), Güemes 3450, (3000) Santa Fe, Argentina. rdondo@santafe-conicet.gov.ar

[‡] Laboratorio de Fermentaciones. Facultad de Bioquímica y Ciencias Biológicas, Universidad Nacional del Litoral, Paraje El Pozo s/n, (3000), Santa Fe, Argentina

Abstract— The dynamics of production and purification of ethanol from sorghum lignocellulosic materials by a three stages process was modeled and optimized in this work. The process involves a first stage for hydrolyzing sweet sorghum bagasse; a second stage for fermenting the generated sugars and a third stage for the separation of ethanol. Kinetic and distillation equations were embedded into macroscopic balances in order to derive a mathematical model used to solve a three-stage optimal control problem. The aim was to maximize the process productivity by optimally managing the controlled flows between units and by optimally fixing switching times between the process stages.

Keywords— multi-stage optimal control; sorghum bagasse; hydrolysis; fermentation; distillation.

I. INTRODUCTION

Bioethanol is the most widely used biofuel and the most promising alternative to fossil fuels. It is also considered clean because of its inherent characteristics of low pollutant (Andrianantenaina and Ramamonjisoa, 2016). Most bioethanol is produced from sucrose containing or starch-based feedstocks. Crop-based bioethanol imposes an adverse effect on global food supply and a sustainable alternative feedstock which can be used for non-crop bioethanol is lignocellulosic biomass such as rice straw, wheat straw, corn stover, switchgrass, sugarcane bagasse and sorghum bagasse. Lignocellulose mainly consists of cellulose, hemicellulose and lignocellulose. Lignocellulosic bioethanol has not yet been produced on a commercial scale due to lack of cost-effectiveness. Nevertheless, the use of lignocellulosic feedstock is considered renewable, since the carbon released to the environment is captured again by the growth of new crops. Comprehensive efforts are required to reduce costs and maximize the profit throughout the whole process. In general, the productivity of growth-associated products in a chemostat is higher than in a batch reactor but this is not always the case with ethanol production (Shuler and Kargi, 2002). Chemostats outperform batch fermenters in ethanol production from glucose alone as cells grow relatively fast but ethanol productivity from mixed sugars in batch cultures is about two to three times higher than in continuous cultures (Song *et al.*, 2012). The productivity of batch fermenters can be further improved by feeding media leading to the use of fed batch fermenters. Also,

the separation of lignocellulosic bioethanol from the culture may strongly affect the process productivity. Increasing the productivity of the whole process should be a preferred target over optimizing individual stages. Modelling is a nontrivial part of optimization aimed at increasing the productivity of a process. This is because a representation adequately predicting the response of the process to all admissible discrete decisions and continuous controls is necessary to optimize it. The optimization of a whole biochemical process would include a multi-stage optimal control problem involving change of dynamics and control variables on several stages because batch and semi-continuous process may involve non-smooth, switched optimal control problems. These problems were mainly researched for aerospace applications but examples from chemical engineering started to appear during the last decade. See for example De Prada *et al.* (2009) and Ni *et al.* (2015). They can be described as follows: given a set of P stages $p \in [1, \dots, P]$, minimize the cost functional defined by:

$$J = \sum_{p=1}^P G(x_p(t_f), x_p(t_0)) + \sum_{p=1}^P \int_0^{t_f} F(x_p(t), u_p(t)) dt, \quad (1)$$

subject to the dynamic constraints:

$$\frac{dx}{dt} = f_p(x_p(t), u_p(t)), \forall p = 1, \dots, P \quad (2)$$

inequality path constraints:

$$C_p^{Min}(t) \leq C(x_p(t), u_p(t)) \leq C_p^{Max}(t), \forall p = 1, \dots, P \quad (3)$$

boundary conditions:

$$\phi_p^{Min}(t) \leq \phi(x_p(t), u_p(t)) \leq \phi_p^{Max}(t), \forall p = 1, \dots, P \quad (4)$$

and the linkage constraints:

$$L_s^{Min} \leq L_s(x_p^{ls}(t), p_p^{ls}, t_p^{ls}; x_p^{rs}(t), p_p^{rs}, t_p^{rs}) \leq L_s^{Max} \quad (5)$$

where $x_p(t)$, $u_p(t)$ and t are respectively the state variables, the control variables and the time in stages $p = 1, \dots, P$; L is the number of pair of stages to link and $s = 1, \dots, L$ are the “left” and “right” stage-numbers respectively (Betts, 2001).

This work is concerned with the numerical derivation of optimal time-profiles for the control variables of a sequential production and separation process for ethanol production from sorghum bagasse and the optimal switching times between hydrolysis, fermentation and distillation stages.

II. MODELS OF THE PROCESS' STAGES

Several ways to generate ethanol from lignocellulosic residues of sweet sorghum are possible but we restrict this numerical study to the enzymatic hydrolysis of

grinded sorghum bagasse with cellulase enzyme; the posterior fermentation of generated sugars by *Saccharomyces cerevisiae* and a final semi-batch distillation stage. The sequential process involves a hydrolysis reactor linked to a separated fermentor as shown in Fig. 1. The feed added to the later reactor contains glucose and some other fermentable sugars arising from the hydrolysis of sorghum bagasse in the former reactor. Afterwards, filtering is performed to feed the aqueous ethanol-solution to the boiler of a distillation column. Since this work presents the numerical application of multi-stage optimal control, materials and methods used to derive experimental information are just referenced.

A. Hydrolysis kinetics

Lignin is a recalcitrant source of carbon compounds that may be decomposed via pretreatment and hydrolysis into a spectrum of sugars in which glucose and xylose are the first and second most dominant (Song *et al.*, 2012). Joris (2015) and Duarte (2018) researched alternatives for identifying high yield and high conversion-rates hydrolytic enzymes to hydrolyze sweet sorghum bagasse. From these studies we took kinetic data for hydrolyzing the bagasse by cellulase enzyme (FibreZyme® G4, Dyadic's, USA) and performed a least-squares regression in order to determine parameter values listed in Table 1. Kinetic equations used to characterize this hydrolysis are the following:

$$r_M^h = -Y_{S/M}\gamma \frac{M}{M+k_1} \quad (6)$$

$$r_S^h = \gamma \frac{M}{M+k_1} \quad (7)$$

where r_M^h is the rate of depletion of lignocellulosic materials, r_S^h is the glucose production rate, M is a variable representing an non-dimensional concentration of hydrolysable sugars into lignocellulosic solids, γ the maximum specific hydrolysis rate, k_1 is the saturation constant and $Y_{S/M}$ is the observable yield of glucose on the lignocellulosic material.

B. Fermentation kinetics

Sugars generated in the above stage are converted to bioethanol by fermentation. An industrial strain of *Saccharomyces cerevisiae* LFF-S04 available on *Laboratorio de Fermentaciones, Facultad de Bioquímica y Ciencias Biológicas, Universidad Nacional del Litoral (FBCB - UNL)*, was used by Duarte (2018) to characterize the fermentation of the hydrolysate generated during the previous stage. Although several fermentable sugars are present in the hydrolysate, glucose is the main product and also the limiting substrate for the biomass growth rate. Kinetic rates are characterized by the following equations:

$$r_X = \mu_{max} \frac{S_f}{k_S+S_f} \left(1 - \frac{P}{k_P}\right) X \quad (8)$$

$$r_P = a\mu_{max} \frac{S_f}{k_S+S_f} X \quad (9)$$

$$r_S = -\frac{1}{Y} \mu_{max} \frac{S_f}{k_S+S_f} X \quad (10)$$

Rates r_X , r_P and r_S are respectively the biomass growth rate; the ethanol production rate and the glucose con-

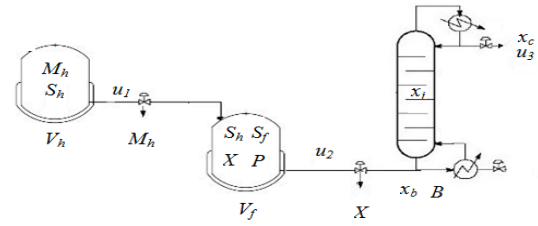


Fig. 1: Schematics of the train

sumption rate. In kinetic Eqs. (8)-(10), S is the glucose concentration, X is the biomass concentration and P is the ethanol concentration; μ_{max} is the maximum specific biomass growth rate; k_S is the Monod constant on glucose; k_i is an inhibition constant considering the braking effect of ethanol on the biomass growth rate; a is the growth-associated Luedeking-Piret specific production rate and Y is an observed lumped yield of products (biomass and ethanol) on glucose. Also, a least squares regression was performed to determine parameter values listed in Table 1.

C. Distillation dynamics

Although other options are feasible, ethanol from aqueous solutions, like fermentation cultures, is usually separated by standard techniques like filtering and distillation. There are quite standardized mathematical representations for these separation techniques. We utilize the model by Logsdon and Biegler (1993) for a trays column which considers the following assumptions: feeding an aqueous mixture at saturation temperature to the boiler; non-ideal vapor-liquid relationships; negligible vapor holdup in each tray and in the boiler; constant vapor flow and constant liquid holdup in trays and in the condenser; theoretical trays; constant operation pressure; adiabatic (i.e. energy balances neglected) column with n stages of equilibrium; and total condensation of the distillate.

III. ASSEMBLING MODELS

The train illustrated on Fig. 1 comprises the hydrolysis reactor, the fermentor and the distillation column and has three main stages. The first stage begins on the hydrolysis reactor and its aim is to generate glucose and several other fermentable sugars. When the hydrolyzable solids are depleted at an unknown time $t_f^{(1)}$, the culture is feed to the fermentor starting the biomass growth and the ethanol production. The fermentation finalizes at an unknown time $t_f^{(2)}$ when fermentable sugars have been practically exhausted. Then, the feeding of the distillation column starts and the separation proceeds until an unknown time $t_f^{(3)}$. Filtering of depleted solids and filtering of biomass are respectively performed to feed the fermentor and boiler. To model the train, kinetic equations linked by yield parameters must be embedded into macroscopic balances equations for both reactors. Furthermore, the dynamics of the distillation column considers that the boiler is feed with the filtered culture. The problem involves three stages; a batch hydrolysis (p_1); fed-

batch fermentation (p_2); and a semi-continuous distillation (p_3); and three control variables: the flow of filtered hydrolysate solution toward the fermentor (u_1); the flow of the filtered culture toward the column boiler (u_2); and the distillate flow (u_3) out of the condenser.

A. Dynamic equations

The dynamics of the whole train is represented by Eqs. (11) to (22). Equations (11)-(12) respectively state the dynamics of sugars-depletion from solids and the glucose production in the hydrolysis reactor. Equations (13) and (14) state the dynamics of the reaction volumes, V_h and V_f , in the hydrolysis reactor and the fermentor respectively. The dynamics of the biomass concentration, X , ethanol, P , and glucose, S_f , in the fermentor are given by Eqs. (15), (16) and (17), respectively. Equation (18) defines the dynamics of the molar fraction of ethanol, x_i , in each tray i . The dynamics of the volume of solution available in the boiler, B , is given by Eq. (19). The molar fractions of ethanol in the condenser, x_c , and in the boiler, x_b , are respectively defined by Eqs. (20) and (21). Equation (22) gives the dynamics of the condensed distillate, D . In this model, binary parameters p_1 , p_2 and p_3 take value 1 whenever their respective stages are active and 0 otherwise; i.e. when hydrolysable solids are depleted then $p_1=0$, $p_2 = 1$, $p_3 = 0$ and when fermentation ends then $p_1=0$, $p_2 = 0$, $p_3 = 1$. Switch-times are determined by the problem solution. Variables y_i , y_c and y_b respectively state the molar fraction of ethanol in the vapor phase on tray i , on the condenser and on the boiler. The liquid flow L in the column is computed as the difference between the vapor flow V and the distillate flow u_3 .

$$\frac{dM_h}{dt} = r_M^h p_1 \quad (11)$$

$$\frac{dS_h}{dt} = r_S^h p_1 \quad (12)$$

$$\frac{dV_h}{dt} = -u_1 p_2 \quad (13)$$

$$\frac{dV_f}{dt} = u_1^f p_2 - u_2 p_3 \quad (14)$$

$$\frac{dX}{dt} = \left(r_x - u_1^f \frac{X}{V_f} \right) p_2 \quad (15)$$

$$\frac{dP}{dt} = \left(r_p - u_1^f \frac{P}{V_f} \right) p_2 \quad (16)$$

$$\frac{dS_f}{dt} = \left(r_S^f - u_1^f \frac{(S_h - S_f)}{V_f} \right) p_2 \quad (17)$$

$$\frac{dx_i}{dt} = \left(\frac{L(x_{i-1} - x_i) + V(y_{i+1} - y_i)}{M_h} \right) p_3, i = 1, \dots, n_{trays} \quad (18)$$

$$\frac{dB}{dt} = (u_2^f + L - u_1^f) p_3 \quad (19)$$

$$\frac{dx_c}{dt} = \left(\frac{V}{M_{hc}} (y_1 - y_c) \right) p_3 \quad (20)$$

$$\frac{dx_b}{dt} = \frac{1}{B} \left(u_2^f (x_f - x_b) + L(x_h - x_b) - V(y_b - x_b) \right) p_3 \quad (21)$$

$$\frac{dD}{dt} = u_3 p_3 \quad (22)$$

Feeding flows u_1^f and u_2^f are respectively related to u_1 and u_2 by algebraic equations to be next defined.

B. Algebraic equations

Vapor-liquid equilibrium data are computed by interpolation between points provided by a table expressed as:

$$y_i = y(x_i) \quad (23)$$

The filtering factor c_1 given by the volume of filtered solids-free solution feed to the fermentor per liter of non-filtered hydrolysate is computed by:

$$c_1 = \frac{1000 - 0.79M^h(t_0^{(1)})}{1000} y(x_i) \quad (24)$$

where $M^h(t_0^{(1)})$ is the initial mass of hydrolyzable material per liter in the hydrolysis reactor. The filtering of solids from the hydrolysate implies that the glucose concentration on the solids-free solution G_1^f and the flow to the fermentor u_1^f are respectively given by:

$$S_h^f = S_h / c_1 \quad (25)$$

$$u_1^f = c_1 u_1 \quad (26)$$

The second filtering operation is performed to separate biomass from the culture fed to the boiler. So, the filtering factor c_2 given by the volume of biomass-free solution per liter of non-filtered culture is computed by:

$$c_2 = \frac{1000 - X(t_f^{(2)})}{1000} \quad (27)$$

This implies that ethanol concentration in the biomass-free solution P_f would be given by:

$$P_f = P / c_2. \quad (28)$$

Since vapor-liquid equilibrium data are expressed in molar fractions, the following expressions must be computed to calculate the molar fraction of ethanol and the molar feeding flow to the boiler:

$$x_f = \frac{P_f / 46}{P_f / 46 + (1000 - X - P_f) / 18}. \quad (29)$$

$$u_2^f = 1e^{-3} \left(P_f / 46 + (1000 - X - P_f) / 18 \right) u_2. \quad (30)$$

Sugars concentration in this flow is assumed negligible because they have been exhausted in the fermentor.

C. Path, state control and end constraints

Optimal control of batch distillations usually involves the maximization of the quantity of distillate subject to purity constraints. The inequality imposing a minimum molar fraction of ethanol in the distillate is:

$$x_c^{min}(t^{(3)}) \geq x_c. \quad (31)$$

Also, a depletion constraint is imposed to the molar fraction of ethanol in the solution on the boiler at the final distillation time:

$$x_b(t_f^{(3)}) \leq x_b^{min}. \quad (32)$$

Both constraints are applied just to the stage p_3 of the problem. Also, limits to the achievable values of some states must be imposed. Here the following constraints must be considered:

$$0 \leq V_h(t^{(2)}) \quad (33)$$

$$0 \leq V_f(t^{(2)}) \leq V_f^{max} \quad (34)$$

$$0 \leq B(t^{(3)}) \leq B^{max} \quad (35)$$

Equation (33) set the lower bound to the hydrolysis reactor. Equation (34) states that the culture volume in the fermentor is a nonnegative variable which must not exceed the reactor-vessel capacity and Eq. (35) imposes the dome capacity as the upper bound to the volume of filtered culture in the boiler. Flows are constrained by Eqs. (36) to (38). Bounds u_1^{max} and u_2^{max} are technical

constraints stating the maximum flow between units. Since the vapor flow in the column is considered constant, it imposes an upper bound to the distillate flow. The liquid flow is the difference between the vapor flow and control variable $u_2(t^{(3)})$.

$$0 \leq u_1(t^{(2)}) \leq u_1^{max} \quad (36)$$

$$0 \leq u_2(t^{(3)}) \leq u_2^{max} \quad (37)$$

$$0 \leq u_3(t^{(3)}) = V_f - L_f(t^{(3)}) \leq V_f \quad (38)$$

D. Objective function

As the hydrolysis is an autonomous process, no objective function is considered for this stage and as increasing the productivity of the whole process is the target, the following objectives are stated for the following stages:

1. Stage 2: Maximum ethanol productivity in the fermentor:

$$\max J^{(2)} = \frac{P(t_f^{(2)})V(t_f^{(2)})}{t_f^{(2)}} \quad (39)$$

2. Stage 3: Maximum distillate productivity:

$$\max J^{(3)} = \frac{D(t_f^{(3)})}{t_f^{(3)}} \quad (40)$$

The problem is a free final-time one defined by the sum of three free-time subproblems. The hydrolytic reaction autonomously evolves until time $t_f^{(1)}$ when the feeding of the fermentor starts. The fermentor is then feed with the hydrolysate in optimal fashion until time $t_f^{(2)}$. Then, the feeding of the boiler starts and the distillation proceed until the final process time $t_f^{(3)}$. The global productivity is defined as the sum of $J^{(2)}$ and $J^{(3)}$ (in gP/h).

IV. MULTI-STAGE OPTIMAL CONTROL OF THE TRAIN

GPOPS was developed in response to a demand for software able to solve complex multi-stage optimal control problems. Its freeware 5.2 version implementing the Radau pseudospectral collocation method (Rao *et al.*, 2012) was employed in this work. Pseudo-spectral methods are a special class of orthogonal collocation methods discretizing both control and states variables. A detailed description of the algorithm implemented by GPOPS can be found in Rao *et al.* (2014). A nominal problem defined by parameters summarized in Table 1 was solved in a 2.0 GHz 16 GB RAM PC. Kinetic and yield parameters for the hydrolytic production of glucose and isomers from Sorghum bagasse with cellulase enzyme and for ethanol production on this hydrolysate with *S. cerevisiae* were derived from experimental information obtained in the Laboratorio de Fermentaciones (FBCB – UNL). Summarized details about materials and methods are reported in Joris *et al.* (2017). Non-ideal vapor-liquid water-ethanol equilibrium data were gently provided by Dr. José Espinoza and coworkers from INGAR (Universidad Tecnológica Nacional – CONICET). The value $x_c^{min}(t^{(3)})$ was considered constant along the last stage. A higher purity value was not considered because of the energetic inefficiency inducted by high reflux ratios necessary to reach

such values. Usually, the obtained distillate is subject to a subsequent purification stage in another smaller distillation column. The output generated for this nominal problem states that the optimal quantity of distillate is $D(t_f^{(3)}) = 2.256$ kmol (104.7 kg). Optimal switch time between the hydrolysis stage and the fermentation stage is $t_f^{(1)} = 10.02$ h while the optimal switch time between the fermentation stage and the distillation stage is

Table 1. Parameter values for the nominal problem.

Parameter type	Parameter	Value			
Yields	$Y_{S/M}$ (g S/g M)	6.550			
	Y (g X/g S)	1.126			
Kinetics	γ (h ⁻¹)	0.039			
	k_1 (g M)	0.010			
	μ_{max} (h ⁻¹)	0.259			
	k_S (g S)	10.00			
	k_P (g P)	51.37			
	k_I (g M)	5.000			
	a (g P/10 ⁶ cells X)	0.655			
Distillation	V_f (kmol/h)	0.600			
	M_h (kmol)	0.30			
	M_{hc} (kmol)	0.90			
	n	4			
	x_c^{min}	0.50			
State bounds	V_{Max} (l)	1000			
	B_{Max}	∞			
Control bounds	u_2^{Max} (l/h)	250			
	u_2^{Max} (l/h)	100			
	u_3^{Max} (kmol/h)	0.6			
End constraint	X_b^{min}	0.002			
Initial conditions					
	($p = 1$)	($p = 2$)	($p = 3$)		
M (g/l)	280	X (g/l)	0.4	x_b	0.012
S_h (g/l)	0	P (g/l)	0.0	x_i (1,...,4)	equilib
		S_F (g/l)	10	x_c	w.boiler
		V (l)	100	B (kmol)	0.807
				D (kmol)	0.0

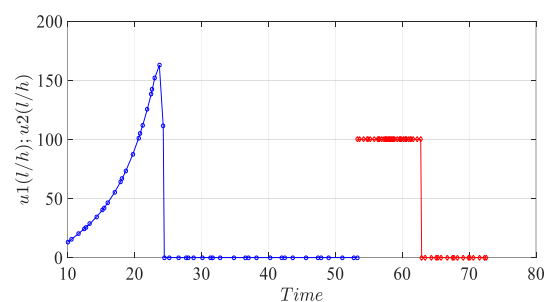


Fig. 2.a: Optimal trajectories for flows $u_1(t)$ and $u_2(t)$.

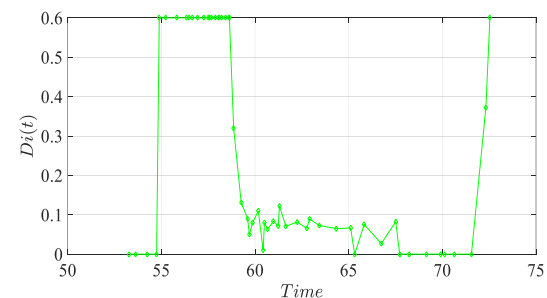
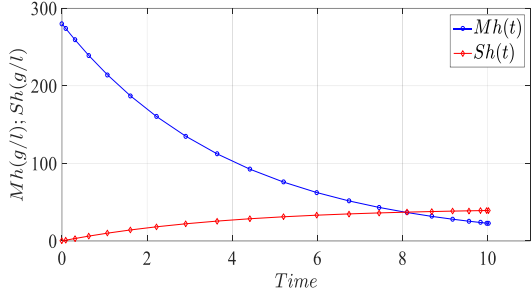
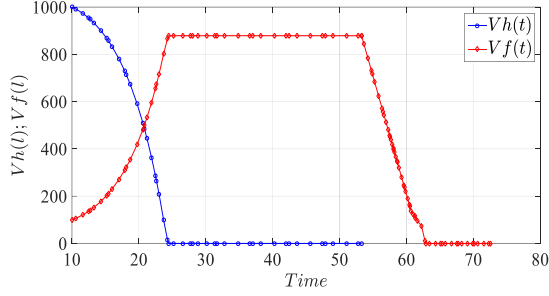
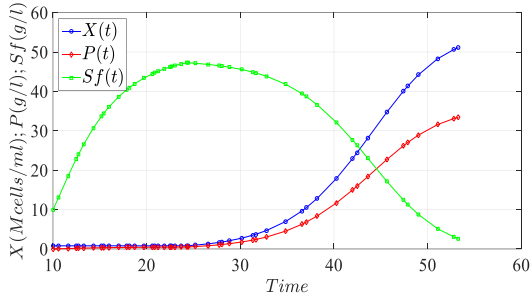
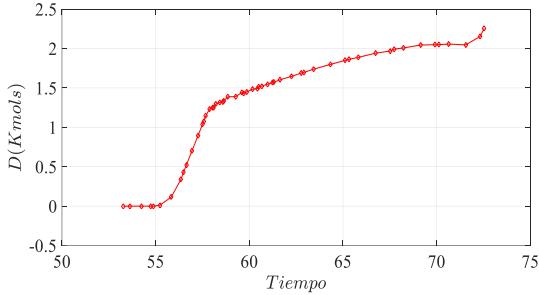
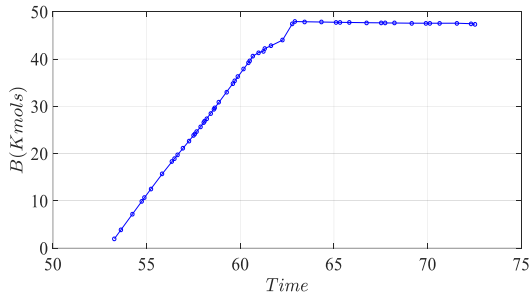


Fig. 2.b: Optimal distillate flow $u_2(t)$.


 Fig. 3.a: Dynamics of $M_h(t)$ and $S_h(t)$.

 Fig. 3.b: Dynamics of reaction volumes $V_h(t)$ and $V_f(t)$.

 Fig. 3.c: Dynamics of $S_f(t)$, $X(t)$ and $P(t)$.

 Fig. 3.d: Dynamics of the distillate $D(t)$.

 Fig. 3.e: Dynamics of the boiler' volume $B(t)$.

$t_f^{(2)} = 53.28$ h and the final process time is $t_f^{(3)} = 72.54$.

Optimal trajectories for control variables are summarized in Figs. 2. Evolution of states according the optimal

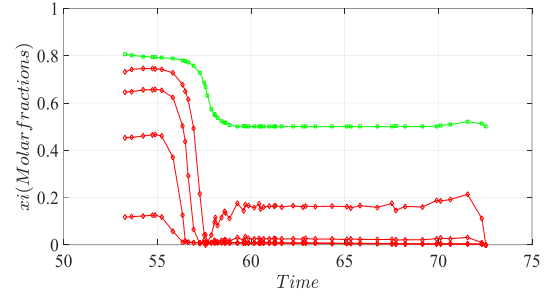
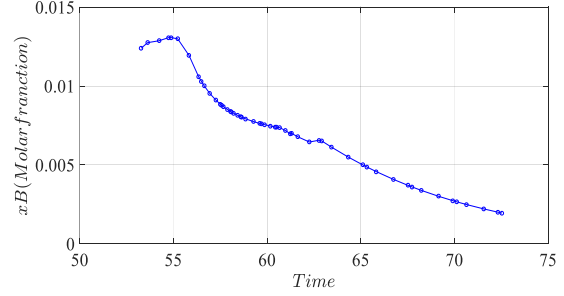

 Fig. 3.f: Dynamics of $x_i(t)$ and $x_c(t)$.

 Fig. 3.g: Dynamics of molar fraction $x_b(t)$.

Table 2 Switching times, objective functions and distillate volume for the nominal and perturbed problems.

Nominal problem ($\gamma = 0.039 \text{ h}^{-1}$; $\mu_{max} = 0.259 \text{ h}^{-1}$; $a = 0.655$)						
	$t_f^{(1)}$	$t_f^{(2)}$	$t_f^{(3)}$	$J^{(2)}$	$J^{(3)}$	$D(t_f^{(3)})$
	10.02	53.28	71.67	551.44	1.458	104.7
Sensitivity to variations on γ						
γ	$t_f^{(1)}$	$t_f^{(2)}$	$t_f^{(3)}$	$J^{(2)}$	$J^{(3)}$	$D(t_f^{(3)})$
0.03	11.89	55.22	74.15	524.96	1.610	104.0
0.05	8.28	51.49	73.91	577.65	1.440	106.4
Sensitivity to variations on μ_{max}						
μ_{max}	$t_f^{(1)}$	$t_f^{(2)}$	$t_f^{(3)}$	$J^{(2)}$	$J^{(3)}$	$D(t_f^{(3)})$
0.20	10.79	66.75	85.81	445.48	1.224	105.1
0.30	9.59	46.98	66.64	620.60	1.555	103.5
Sensitivity to variations on a						
a	$t_f^{(1)}$	$t_f^{(2)}$	$t_f^{(3)}$	$J^{(2)}$	$J^{(3)}$	$D(t_f^{(3)})$
0.50	10.34	51.67	70.27	445.30	1.316	92.3
0.80	9.37	54.31	76.68	628.75	1.518	116.3

switching times and control trajectories are depicted in Figs. 3.

Note that some numerical instability in the optimal distillate flow can be observed. This is a quite common phenomena observed in optimal control of batch distillations, as noted by Logsdon and Biegler (1993), which seems not to considerably distort the evolution of the quantity of distillate depicted in Fig. 3.d.

Optimal control has been used mostly in fields where process models are well known and, but it has had fewer acceptances in biotechnology, where model uncertainties can be significant. In order to study the effect of variations on parameters γ , μ_{max} and a , we performed a brief sensitivity study by varying these parameters. Results are summarized in Table 2.

From data summarized in Table 2, the following conclusions can be stated: (i) Although stage 1 evolves spontaneously, the final stage time $t_f^{(1)}$ may change according

the dynamics of subsequent stages. (ii) Stage 2 time-length ($t_f^{(2)} - t_f^{(1)}$) depends mainly on specific biomass growth rate but its impact on the distillate value $D(t_f^{(3)})$ is almost negligible. (iii) The distillate value $D(t_f^{(3)})$ is strongly impacted by variations in the Luedeking-Piret specific production rate but its impact on the final process time is rather minor. (iv) Variation on the specific hydrolysis rate γ affect in the duration of the hydrolysis stage but the impact in remaining performance parameters is almost negligible.

V. CONCLUSIONS

A three-stage model for optimizing a train of a hydrolysis reactor, a fermentor and a distillation column was used to optimize units' control variables and switching times between stages. The model involves experimental information for the hydrolytic production of glucose and isomers from Sorghum bagasse with cellulase and the kinetics of ethanol production from generated sugars by *S. cerevisiae*; and bibliographic information for distillation parameters. Kinetic equations and distillation dynamics equations were introduced into macroscopic balances for modeling a train involving three control variables: the flow of hydrolysate toward the fermentor, the flow of the filtered culture from the fermentor toward the boiler of the distillation column and the distillate flow. Since this multi-stage (bio)chemical process involve switching dynamics and change of control variables along the time, stages time-lengths should not be independently fixed. So, control variables were optimally profiled and time-scheduled by using GPOPS 5.2. As a consequence, optimal flow profiles and switching times were computed. A brief sensitivity research on the effect of the variation of main kinetic parameters was also performed. A more compressive sensitivity research based on stochastic programming should be performed but this is out of the scope of this work. Multi-stage process involving switching dynamics and change of control variables are common in (bio)chemical engineering but optimization of such processes arise recently. In this regard, the optimization of the whole train aimed at maximizing the overall productivity shows that separately optimizing independent units is not a good option. The results show that nowadays there are no big obstacles in optimizing mathematical representations of multi-stages process because modern optimal control tools can handle multi-stage mathematical models.

REFERENCES

Andrianantenaina, M.H. and Ramamonjisoa, B.O.A. (2016) "Hydrous ethanol as a renewable household fuel for low-income country: case study for Madagascar," *Lat. Am. Appl. Res.*, **46**,121-126.

- Betts, J.T. (2001) *Practical Methods for Optimal Control Using Nonlinear Programming*, SIAM Press, PA, USA.
- de Prada, C., Grossmann, I., Sarabia, D. and Cristea, S.A. (2009) "Strategy for predictive control of a mixed continuous batch process," *J. Process Control*, **19**, 123-137.
- Duarte, F. (2018) *Control óptimo de procesos biotecnológicos de múltiples etapas. Aplicación a la producción de etanol a partir de hidrolizados enzimáticos de materiales lignocelulósicos*, Tesis de Grado. Fac. de Bioquímica y C. Biológicas. Universidad Nacional del Litoral, Argentina (2018).
- Joris, G. (2015) *Modelado y optimización de fermentaciones alcohólicas desarrolladas a partir de hidrolizados enzimáticos de materiales lignocelulósicos*, Tesis de Grado. Fac. de Bioquímica y C. Biológicas. Universidad Nacional del Litoral, Argentina.
- Joris, G., Duarte, F., Beccaria, A. and Dondo, R. (2017) "Optimizing ethanol production from lignocellulosic-materials of sorghum by a sequential hydrolysis and fermentation methodology," *Simpósio de Informática Industrial SII*, Córdoba, Argentina.
- Logsdon, J. and Biegler, L. (1993) "Accurate Determination of Optimal Reflux Policies for the Maximum Distillate Problem in Batch Distillation," *Ind. Eng. Chem. Res.*, **32**, 692-700.
- Ni, Y., Biegler, L., Villa, C. and Wassick, J. (2015) "Discrete time formulation for the integration of scheduling and dynamic optimization," *Ind. Eng. Chem. Res.*, **54**, 4303-4315.
- Rao, A., Benson, D., Darby, C., Francolin, C., Patterson, M., Sanders, I., and Huntington, G. (2012) *User's Manual for GPOPS; Version 5.2*. Gainesville, USA.
- Rao A., Benson, D., Darby, C., Patterson, M., Francolin, C., Sanders, I. and Huntington, G. (2014) "Algorithm 902: GPOPS, a Matlab software for solving multiple-phase optimal control problems using the gauss pseudospectral method," *ACM Trans on Math. Soft.*, **22**, 1-39.
- Shuler, M. L. and Kargi, F. (2002) *Bioproc. Eng. Basic Concepts*. Prentice-Hall, Inc. U.S.A.
- Song, H., Morgan J. and Ramkrishna D. (2012) "Towards increasing the productivity of lignocellulosic bioethanol: rational strategies fueled by modeling," *Bioethanol*, Lima. M.A.P., ed., InTech, Rijeka, Croatia.

Received: August 1, 2018

Sent to Subject Editor: May 9, 2019

Accepted: March 4, 2020

Recommended by Subject Editor: Mariano Martín Martín